Numerical simulation of a vibratory roller on cohesionless soil

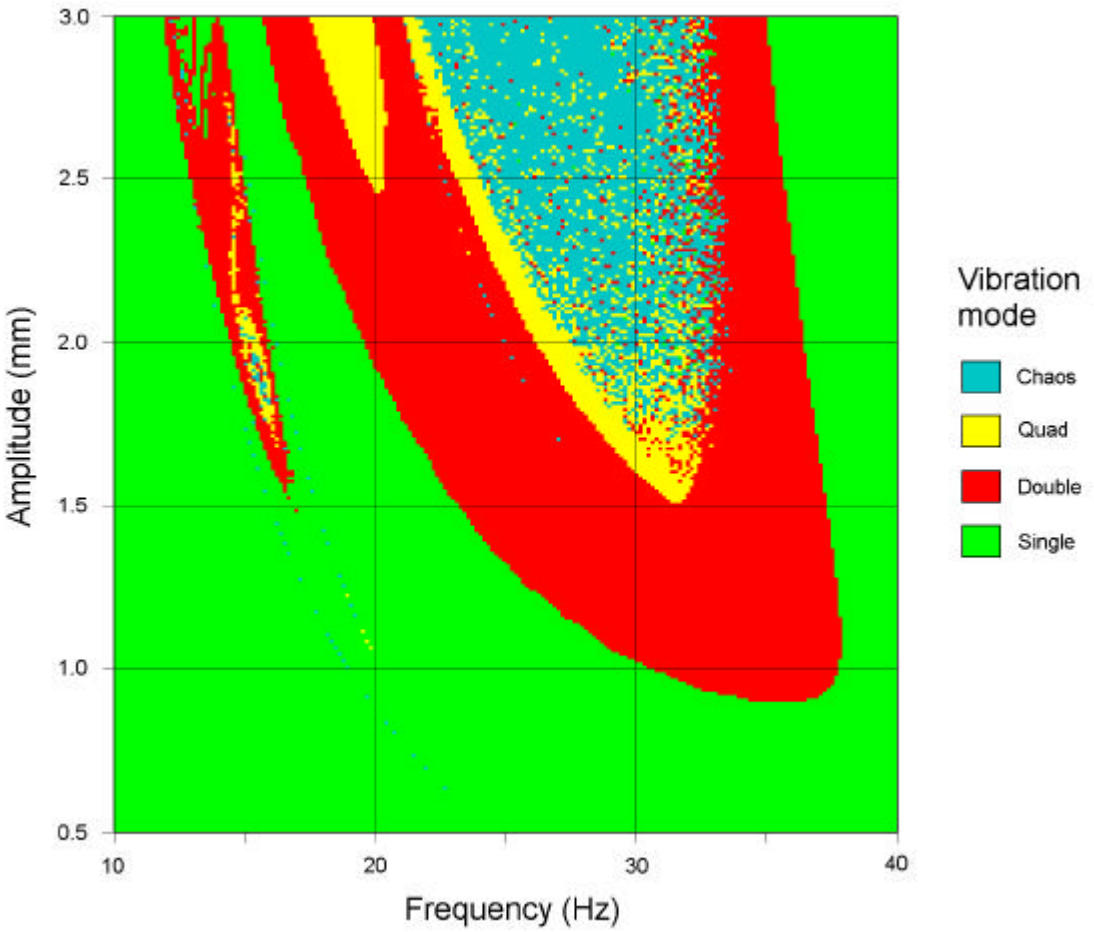

Åke Sandström, 9411

GEODYNAMIK

Numerical simulation of a vibratory roller on cohesionless soil

Åke Sandström, Geodynamik AB

Abstract

Compaction of soil by a vibratory roller is a complex process. Various soil properties and roller parameters interact making the dynamic drum/soil system a highly non-linear one. The reasons for non-linearity are the plastic deformations in the soil and the fact that the contact between the drum and the soil may be lost for a portion of the cycle.

Prediction of the dynamic behaviour of a vibrating drum acting on a soil layer is important for several reasons. It can be used for optimising the parameters of the roller and also to study the limits for stable vibration and to evaluate different compaction meter systems.

A numerical model of the drum/soil system is described in the paper. The model takes into account the most important factors influencing the dynamics of the system. The soil is characterised by an elastic parameter comparable to the shear modulus of a homogenous isotropic half space and the plastic effect in the compaction zone is modelled by a second parameter. The design of the model is described and results are presented for a few examples. Predicted accelerations of the drum, force/displacement relations, maximum force generated by the drum and vibration stability are presented. CMV-values are also calculated and displayed as function of the compaction state.

Introduction

Vibratory rollers have been used for many years and the design has evolved step by step from towed types to self propelled rollers of different weight classes (Forssblad [7]). The drums are smooth for compaction of gravel or rock-fill. Sheepsfoot or padfoot drums are used for clay and other cohesive material. For the compaction of thin gravel layers and asphalt paving the tandem type of roller having two smooth drums is very common. The oscillatory roller is a new type of roller, gaining popularity for use both in soil and pavement compaction.

The optimum design of a vibratory roller poses some difficult problems. The roller should compact efficiently on different types of soils and in different stages of compaction from loose to fully compacted. It is well known that a drum bouncing on the soil surface can enter undesirable vibration states like double jump and rocking motion. Existing vibratory rollers normally have one or two

different frequency/amplitude settings and therefore represent a compromise regarding the compaction efficiency under various soil conditions.

Rollers evolved step by step in a trial and error process. It was however soon realised that there is a need for theoretical modelling and a number of investigations have been performed with the aim of increasing the theoretical basis for the design of vibratory rollers. The first models were linear and aimed at studying basic phenomena as conditions for drum lift off and relations between the eccentric force and the force applied to the soil (Machet[15], Yoo and Selig [28]).

Work was started at Geodynamik around 1980, with the aim of developing a computer simulation model that could take into account the non-linearities involved in the drum/soil system and the important parameters of the roller. The aim was to create a tool for roller design, especially for the development of automatically controlled rollers and for the study of compaction meters. It was considered important that the model had a simple basic structure that could be extended to include different aspects of the roller and the soil. The parameters of the model should be understandable, measurable and comparable to standard parameters in soil mechanics. A simulation model was developed along these lines and it was used in practice during the eighties. The model was used primarily for parameter studies on existing rollers in consultancy work for different roller manufacturers.

The basic idea behind the simulation model is the following. When loaded dynamically by a cylindrical roller drum, the soil is modelled by two separate parts, acting in series. One part is a plastic one, having a load/displacement relation that can be obtained from conventional bearing capacity theory and the second is an elastic part. The modelling of the elastic part is solved by using results from research on dynamics of foundations.

Work regarding the dynamic loading of an elastic half space has been going on for many decades. These investigations aimed at predicting the dynamics of different structures resting on soil e.g. machine foundation design, earthquake action on buildings and wave action on structures resting on the sea bed. The knowledge has evolved from pure analytical solutions for circular plates resting on an ideally elastic half space [3,20,23] to lumped parameter models [11,14] to numerical schemes for taking into account hysteresis, rate dependence and irreversible deformations in real soil [2]. The methods have also been extended to arbitrarily shaped loading areas and layered soil [5,6,16]. Results from this research is also applicable in the case of dynamic action of a roller drum and is used in the modelling of the elastic part of the simulation model.

Pietzsch [19] developed a model, composed entirely of mass, spring and damper elements. He included non-linear elements and also allowed the drum to lift off from the soil surface. Energy losses by radiation were simulated by an added mass/spring/dashpot system. There are a number of coefficients for the different elements included in the model and they have to be calculated from known soil parameters. This may be difficult since there is no direct correspondence between the element parameters and conventional soil parameters.

A method similar to the one presented in this paper was used by Grabe [9] to simulate the behaviour of a vibrating roller on soil. He however used a different method to model the soil. In addition to an elasticity module for deeper layers, Grabe used the loading stiffness and also the ratio between the loading stiffness and the unloading stiffness as soil parameters.

Static vertical load from a cylinder on a soil surface

1. Plastic deformation

The loading of the flat surface of a thick layer of friction material from a smooth circular cylindrical steel drum of a vibratory roller is considered.

There will be a contact zone, that will undergo plastic deformation down to a certain depth, the extent of which is dependant on the strength of the material and of the line load and radius of the drum. The width and depth of the contact zone will initially be zero and there will therefore always be a zone of soil failure. The extent of the failure zone will increase as the load on the cylinder is increased. An equilibrium will be reached when the total static line load of the roller is applied. The total vertical displacement of the cylinder under influence of the static line load and with respect to the originally flat surface is a characteristic measure of the strength of the soil.

The failure zone is extending downwards to a certain level, that is related to the width of the contact area, the internal friction angle and the density of the soil material.

The problem of calculation of load versus settlement, with regard to plastic effects only, resembles the classical problem of estimating the bearing capacity of a strip or plate foundation. Figure 1. The main difference is that the loading body has a curved surface and that the geometry is changing with increasing load.

The stress distribution under the drum is affected by the radius of the cylindrical loading body and differs from the one present under a flat plate. The effect of this can be expected to be moderate because of the active wedge forming under the contact area. It is assumed that the surface roughness of the cylinder is high enough to prevent sliding at the interface with the soil.

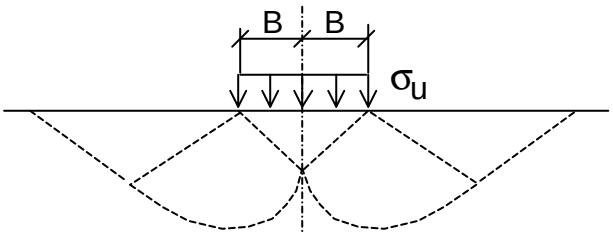

Figure 1: Conventional bearing capacity theory.

The influence of a curved lower surface of a strip foundation was investigated by Széchy[24]. He made laboratory tests to investigate the bearing capacity of rectangular loading bodies having different length/width ratio. Flat, convex and concave concrete bodies were tested on compacted sand and gravel. The results were that the bearing capacity is somewhat reduced for a convex surface compared to a flat one.

The bearing capacity for a strip foundation according to Figure 1 is often expressed as:

$$s_u = cN_c + qN_q + Bg\,N_g \qquad (1)$$

with the bearing capacity expressed as a sum of the contributions by cohesion, surcharge and unit weight of the soil material respectively.

The so called bearing capacity factors N_c, N_q and N_γ are functions of the internal friction angle φ alone.

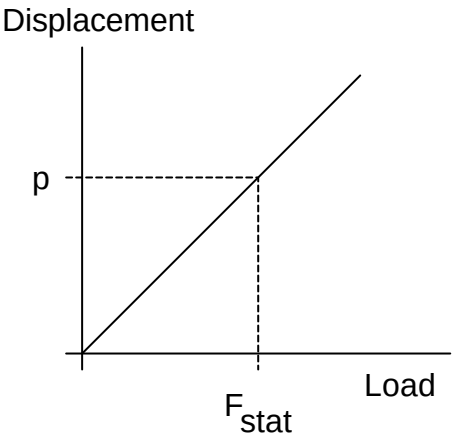

Figure 2: Plastic load/displacement relationship for a cylinder.

Neglecting cohesion and assuming that there is no surcharge, the total load capacity of a rectangular area of width 2B and length W can be written:

$$Q_u = g\,B\,N_g \cdot 2\,BW = const \cdot B^2 \qquad (2)$$

Approximating the cylindrical cylinder with a parabolic cylinder in the contact area, the relationship between the settlement of the cylinder and the mobilised bearing capacity of the plastic layer will be linear.

A plasticity parameter p is defined as the plastic deformation corresponding to the static load . See Figure 2.

2. Elastic displacement

The plastified zone developing under the drum will determine the stress distribution acting at a level below the zone, and it will be different from the one predicted by the theory of elasticity for the contact between a cylinder and a flat surface of an elastic medium. The load will cause displacement of the soil below the plastified zone that is mainly elastic.

In a theoretical sense the word "elastic" applies to a material which recovers completely after the removal of an applied stress. This does not mean that the stress-strain relationship is linear. For the superposition principle to be applicable, however, the stress-strain relationship must be linear and in connection with analytical solutions the material is considered to be "linear elastic".

Soil cannot be considered as an ideal homogeneous isotropic elastic medium having constant values of the elastic constants G and ν. Because of the nature of the formation processes involved, soils in situ are far from homogenous and also far from isotropic. In the context of compaction of soils, the structure is normally built in several layers using locally available material. The quality of the material is generally highest near the final surface or foundation level while deeper layers are built from lower cost material.

The dynamic behaviour of soil material is strongly dependant on

- void ratio or degree of compaction
- strain amplitude
- stress situation
- number of load cycles

The G-modulus determined by conventional geotechnical methods underestimate the actual modulus at small strains. The maximum modulus at small strains can be determined by resonant column tests or in situ seismic methods.

Hardin and Richart [10] determined G-moduli indirectly by measuring shear wave velocities in situ. They present the initial modulus as

$$G_{\max} = C_1 \frac{(C_2 - e)^2}{1+e} \sqrt{\bar{\sigma}_0} \qquad (3)$$

where e = void ratio, $\bar{\sigma}_0$ = mean principal effective stress and C_1, C_2 are parameters that are functions of gradation and grain shape.

For a horizontal homogenous layer, the mean principal effective stress is related to the effective vertical stress as

$$\bar{\sigma}_0 = \left(\frac{1+2K_0}{3} \right) \bar{\sigma}_v \qquad (4)$$

where K_0 is the ratio of lateral to vertical stress.

The effective vertical stress varies with depth and density of the soil material. The value of K_0 generally increases with the degree of compaction.

To be able to model the roller behaviour and it's interaction with the soil, it is necessary to model the load/deformation conditions of the soil as seen downwards from the level just below the plastified contact zone. The deformation condition at this level is the integrated effect of the properties of all the underlying layers. It is not the aim of this investigation to incorporate the wide field of aspects on varying elastic properties with depth and stress/strain level, nor the layering of the soil.

The layers below the contact zone will be modelled as an elastic half space. The values for the elastic soil constants G and ν that should be used are related to the real deformation parameters in the soil mass. The relation is similar to the connection between measured plate load moduli and soil parameters.

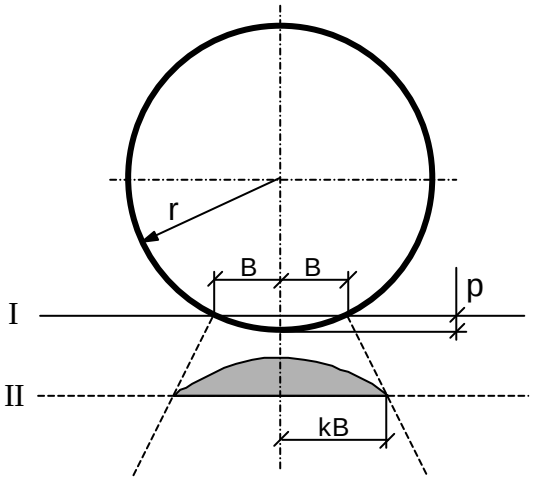

Figure 3: Assumed vertical stress distribution.

The elastic deformation of deeper layers is assumed to be governed by a parabolic load as shown in Figure 3.

The first step is to formulate the displacement for a total vertical static load Q distributed over a rectangular area as shown in Figure 4.

The displacement is calculated by integration of the expression for a point load according to elasticity theory and the result is expressed as a non-dimensional parameter D.

$$D = \frac{\delta G B}{Q(1-\nu)} = \frac{1}{\alpha} \cdot \frac{3}{4\pi} \cdot I(\alpha) \qquad \text{where } \alpha = \frac{L}{B} \qquad (5)$$

$I(\alpha)$ is the expression arising at the integration of the displacement- according to Boussinesq - from the assumed parabolic stress distribution over a rectangular area with length/width-ratio α . The value of the integral can be very closely approximated by:

$$I(\alpha) \approx 0.66 \ln(7.9\alpha) \qquad (6)$$

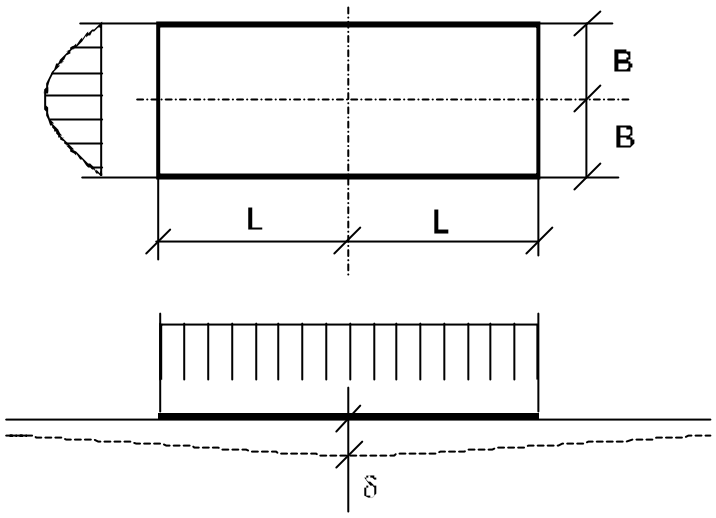

Figure 4: Parabolic load on a rectangular area.

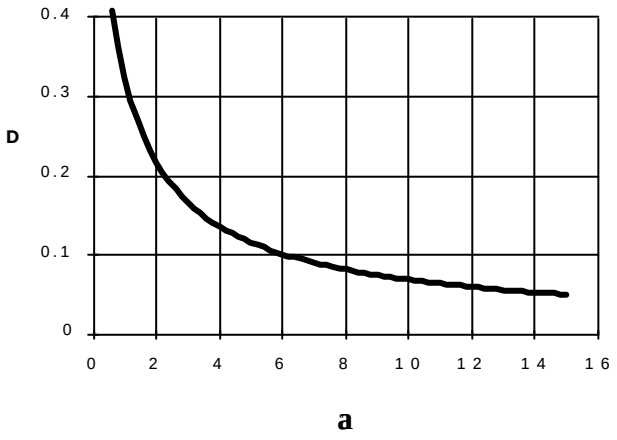

Figure 5: Dimensionless displacement function

The resulting dimensionless expression *D* versus the length/width-ratio α is shown in Figure 5.

The displacement parameter D can be used to calculate the displacement at the centre of a rectangular area when the vertical stress distribution is parabolic along the short axis of the area and constant along the long axis.

A more clear picture of the influence of the shape of the loaded area is obtained if the displacement is compared to the one for a square, keeping the magnitude of the area and the total load constant. This result is shown in Figure 6.

It is assumed that the stress distribution is constant along the whole width of the roller drum. This is an approximation because the drum itself does not deform and therefore produce a constant strain rather than a constant stress. The presence of the plastified contact zone, however evens out the stress variation and the approximation is therefore considered to be justified.

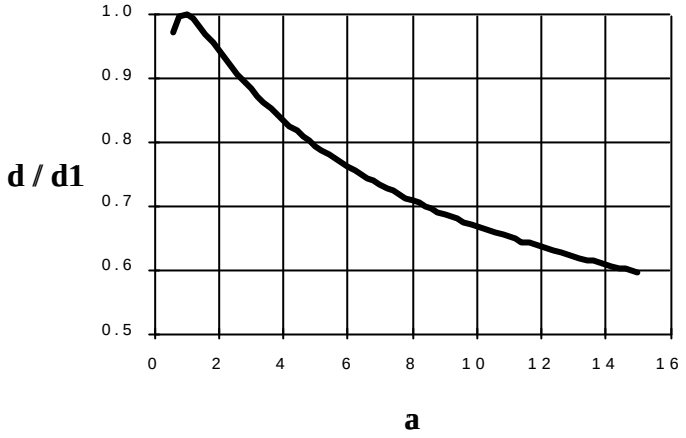

Figure 6:

Displacement at the centre of a rectangular area in relation to a square area. The total load and the size of the area are constant. The load distribution is parabolic along the short axis.

Dynamic vertical load on an elastic half space

Considering a weightless plate resting on an elastic half space, the displacement at the centre of the plate can be expressed as function of the load. When the load is constant, there is a linear relation between the magnitude of the load and the resulting deformation determined by the elastic constants of the continuum, the shape of the loaded area and the stress distribution on the loaded area.

$$z_{se} = \boldsymbol{k} \cdot Q \qquad (7)$$

where $\mathbf{z_{se}}$ is the elastic soil displacement and **Q** is the total load. The factor **k** can be calculated from equation (5).

When the load varies with time the amplitude relation between load and deformation changes, and there is a time lag between the load and the deformation. Energy is flowing away from the loaded area as elastic waves into the medium and along the surface of the half space. The important parameter governing the problem is the speed of shear waves in the medium in relation to the driving frequency and the size of the loaded area. This is expressed as the ratio between a linear dimension of the area and the wavelength of shear waves.

$$a_0 = \frac{d}{v_s / \boldsymbol{w}} \qquad (8)$$

where **d** is a characteristic linear dimension of the loaded area, **w** is the circular frequency

and $v_s = \sqrt{\frac{G}{\boldsymbol{r}}}$ is the shear wave velocity.

The frequency response of the this linear system can be characterised by a complex transfer function of order n expressed in Laplace form as

$$H(s) = H_0 \frac{a_n s^n + a_{n-1} s^{n-1} \mathrm{K} \ +1}{b_n s^n + b_{n-1} s^{n-1} \mathrm{K} \ +1} \qquad (9)$$

The coefficients of Equation (9) are real valued and therefore complex poles and zeroes appear as conjugate pairs. The poles have to be in the negative half of the s-plane for equation (9) to represent a stable system.

The Laplace transform of the displacement can be written formally as the product of H(s) and the Laplace transform of the driving force.

In our case we want to calculate numerically step by step the resulting deformation from a given load input. In order to achieve this, equation (9) is mapped to a z-transform representing a sampled version of the system having a constant time step of Δt. The mapping is made by using a bi-linear transform, equation (10). This means that an ideal integrator (1/s) is represented by a trapezoidal approximation.

$$\frac{1}{s} \rightarrow \frac{\Delta t}{2}\left[\frac{z+1}{z-1}\right] \qquad (10)$$

This mapping converts equation (9) to a rational function of z, which can easily be reformulated as a difference equation relating consecutive samples of the displacement to consecutive samples of the load time series. Starting with a known state of the displacement, it is possible to calculate the displacement step by step for any given time history of loads.

The problem remains to determine the poles and zeroes of the transfer function for the given half space and loading area. This can be achieved by methods common in filter synthesis in electrical engineering. The poles and zeroes of equation (9) are determined by linear programming in order to approximate the frequency response with a sufficient accuracy. The number of poles and zeroes necessary for a sufficient accuracy depend on the complexity of the frequency response function.

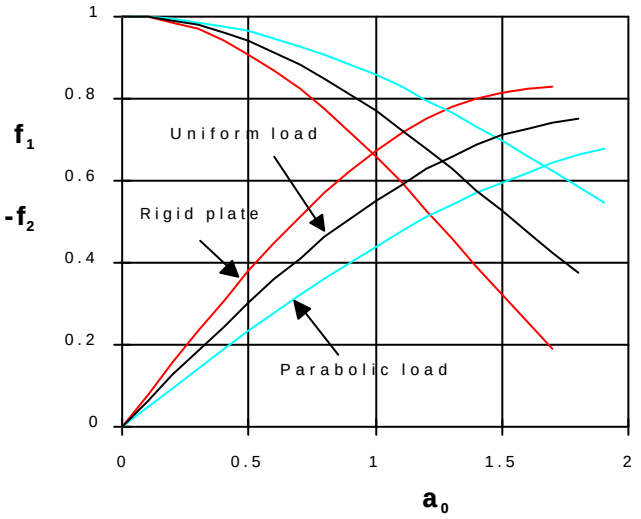

*Figure 7: Compliance functions for a circular plate, **n** = 0.25.*

Analytical solutions of dynamically loaded areas on top of an elastic half space can de found in the literature for vertical, horizontal and rocking mode deformation of circular areas. Different load distributions have also been treated, corresponding to a rigid plate, a uniform load distribution and parabolic load distribution [3,20,23].

Because of the complicated expressions arising, available closed form solutions are limited to circular shapes.

The solutions are expressed as compliance functions often denoted as f_1 and f_2 after Reissner [21]. f_1 is the real part and f_2 the imaginary part of H(s) evaluated along the imaginary s-axis.

Figure (7) shows results compiled by Sung [23] for circular load areas and different load distributions. As pointed out by Richart it seems possible to collapse the curves into one by assigning an "effective radius" for each type of distribution. This would be equivalent to applying different scaling

factors to the horizontal scale for the different load distributions in Figure (7). The effective radius for the rigid plate would be 1.273 r_0 and for the parabolic load it would be 0.75 r_0 to convert to equivalent uniform load cases. Hsieh [11] transformed the Reissner functions into functions containing a spring term and a damping term, both being frequency dependent. His idea was developed further by Lysmer and Richart[14] and others and has been widely used in prediction of the dynamics of different structures resting on soil.

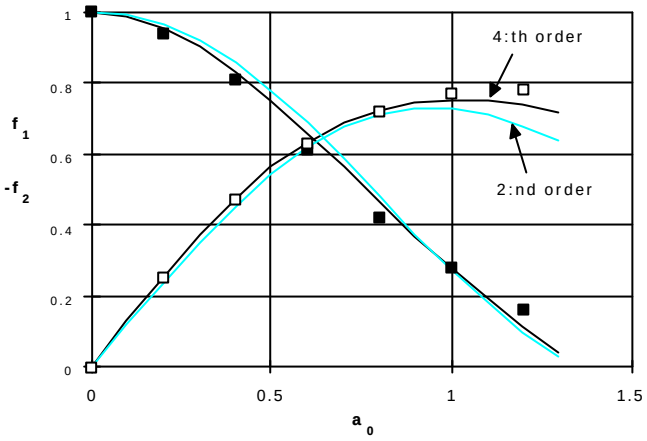

Figure 8: Compliance functions for a rectangular load area. Approximation of solution by Elorduy et al. (points in the diagram) with 2-pole and 4-pole functions.

Non-circular shapes are difficult to treat analytically. Numerical solutions have however been presented e.g. by Dasgupta and Rao [5], Elorduy et al. [6], Meek [16], Veletsos and Verbic [25] and Öner[18]. The most interesting case from a practical point of view is the one with a rectangular load area.

Because of the variation of the elastic properties of the soil with depth as described above, there is a need for methods to estimate the influence of these effects. Dasgupta and Rao [5] made 3D FEM-calculations for cases having linearly increasing G-modulus with depth. Öner [18] calculated equivalent spring constants and damping ratios for cases with spatially varying elastic properties.

Borja [2] included hysteresis, rate dependence and irreversible deformation of the soil in 3D FEM-calculations of circular and square foundations.

Roller simulation program

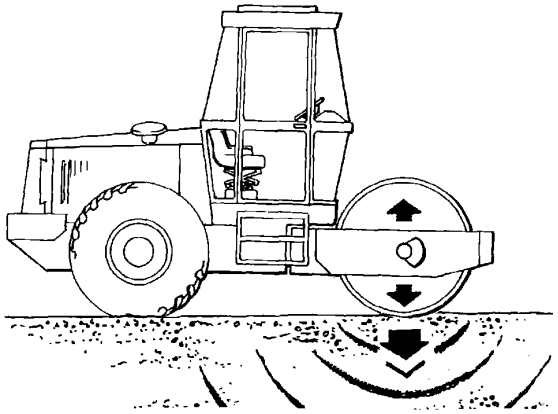

Figure 9: Self propelled vibratory roller.

A system consisting of a vibratory roller compacting a soil layer is fairly complex. A simulation program therefore has to be simplified in many respects and focused on the parameters that are most important for the problem at hand.

The modelling of different details in the roller may be important for the roller designer and may require a modelling of for instance the exciting shaft including the dynamic effects of couplings and the hydraulic motor driving the shaft, while the modelling of the soil may be simplified.

On the other hand, when dealing with the compaction efficiency of a machine, the interaction between the drum and the soil is very important and therefore has to be modelled in greater detail.

A series of different simulation models has developed at Geodynamik over the last 15 years. They were tailored for different needs and the programs have been used for basic research in connection with development of compaction meters and automatic rollers and also for evaluation of the roller designs of different companies.

In this article, the emphasise will be placed on the basic part of the problem, namely the interaction between the cylindrical drum and the soil. The purpose is to demonstrate the basic ideas and possibilities using a simplified model.

A conventional vibratory roller excited by a rotating eccentric mass will be studied. A system with two counter-rotating eccentric masses adjusted for vertical forces can also be investigated with the same model and will give similar results.

Calculations with models taking into account both vertical and horizontal motions as well as rotations of the drum, have shown that there are some horizontal reaction forces at the drum/soil interface. The vertical forces are, however, the most important for the compaction effect and for the other phenomena we are going to study here.

We will therefore deal only with drum/soil forces in the vertical direction and neglect the horizontal drum/soil forces, resulting from the rotation of the drum and the horizontal motion of the drum.

This is at least qualitatively justified by the curve in Figure 10, showing a typical result from calculation of the drum acceleration in vertical direction vs. horizontal direction with time as parameter. The result compares well with results obtained when measuring with biaxial accelerometers on a roller drum.

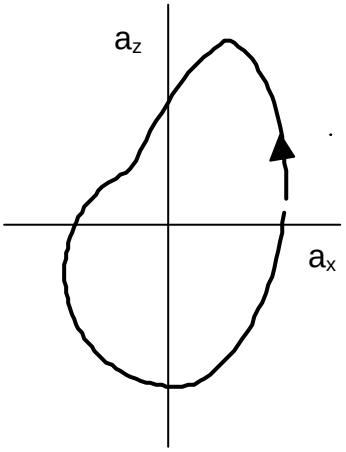

Figure 10: Simulated drum acceleration in horizontal and vertical directions.

The frame of the roller consist of several stiff parts that are connected to each other with more or less soft connecting elements. As seen from the drum, the frame has the main effect of supplying a static load on it, in order to increase the line load on the ground and to enable full exploitation of dynamic compaction force.

The connection between the drum and the frame is normally very soft, the resonance frequency of the frame being of the order of one tenth of the excitation frequency. The damping in the suspension is also generally very low. The transmission of dynamic forces from the drum to the frame is therefore small compared to the other forces acting on the drum during compaction.

1. Roller model

The simplified model of the drum being used is shown in Figure 11.

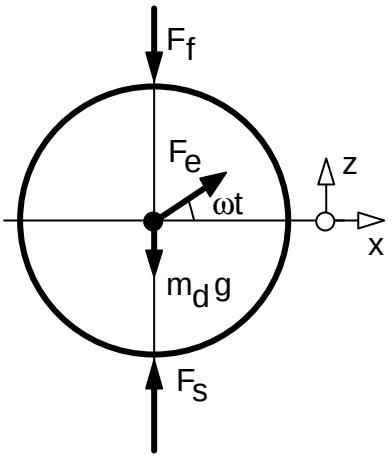

Figure 11: Forces acting on the drum.

F_f is the force acting on the drum from the frame. Only the static part of the force is taken into account.

$F_e(\omega t)$ is the force generated by the eccentric system. It is assumed to be varying harmonically at one single frequency.

m_d is the mass of the drum.

F_s is the reaction force from the soil, which is a complex function of the motion of drum and the deformation of the soil.

All the forces on the drum, except the soil force F_s, can readily be calculated from the masses and from details of the eccentric system.

The motions of the drum in the vertical z-direction and horizontal x-direction are governed by the following equations:

$$m_d \frac{d^2 z}{dt^2} = F_e \sin(\omega t) + F_s - F_f - m_d g \qquad (11)$$

$$m_d \frac{d^2 x}{dt^2} = F_e \cos(\omega t) \qquad (12)$$

2. Soil model

As was outlined above, the deformation properties of soil are very complex especially under dynamic conditions. In addition, there are always plastic deformations taking place under the drum of the roller. It is not realistic to model all the details of a set of layers at all stages of compaction.

The aim was instead to design a numerical model that will enable one to study

- a thick homogenous layer of granular material
- the nearly stationary conditions at the final stage of compaction
- forces and deformations at the drum/soil interface
- the influence of different soil parameters
- the influence of different roller parameters
- the possibilities and limitations of extracting information on soil properties from measured roller parameters.

The real soil layer has to be modelled in such a way, that it describes with sufficient accuracy

- energy consumption through plastification
- flow of energy by elastic waves moving away from the area
- return of energy to the roller

This aim has to be achieved by using as few parameters as possible to describe the soil, and furthermore by using parameters that have a geotechnical meaning and can be estimated for a practical case. This rules out the use of a system of springs, dampers and masses.

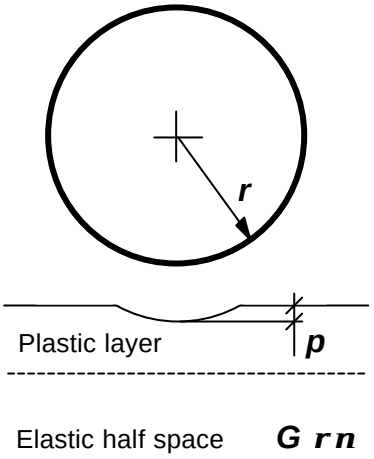

Figure 12: Definitions.

A simple system that meets the requirements consists of a 'plastic layer' on top of an elastic half space. The plastic and elastic effects are in this way separated and attributed to two separate layers. This does not mean however that energy losses are confined to the 'plastic layer' - energy will also be lost in the elastic half space through radiation and internal damping.

The 'plastic layer' will deform according to the actual force applied and is considered to have no mass and no elasticity. It's thickness will actually vary with the magnitude of the contact force. The layer is characterised by a single parameter ***p***, defined as the depth of the remaining indentation created by the roller drum when lowered upon the flat surface with it's static load and than lifted again. See Figure 12. The value of ***p*** is mainly a function of the internal friction angle and density of the soil and of the line load and radius of the drum.

As detailed above, the relationship between the vertical displacement of the roller drum and the force will be close to linear when the cylinder is sinking into an originally flat surface, causing progressive failure of the soil in the contact zone. For moderate deformations, the cylindrical drum surface can be approximated by a parabolic cylinder and the width of the contact area will be increasing as the square root of the vertical displacement. According to conventional bearing capacity theory, the failure load is proportional to the square of the width. The resulting equation describing the deformation of the plastic layer alone is therefore assumed to be:

$$\begin{aligned} \Delta z_{sp} &= -p \cdot \frac{\Delta F_s}{F_{stat}} \qquad \Delta F_s > 0 \\ \Delta z_{sp} &= 0 \qquad\qquad\qquad \Delta F_s \le 0 \end{aligned} \tag{13}$$

where F_{stat} is the total static load acting on the soil surface when the roller is at rest.

The elastic half space assumed for the layers below the 'plastic layer' is loaded by a strip load assumed to have a width equal to a factor ***k*** times the width of the contact area created by the plastic deformation and a length equal to the width of the roller drum. The stress distribution is assumed to be parabolic along the rolling direction and constant in the cross direction. See Figure 3.

The displacement of the elastic half space was expressed above as a transfer function H(s) approximating the Reissner functions for the particular loaded area and stress distribution. The relationship between the displacement and total force is thus formally written as

$$\tilde{z}_{se} = H(s) \cdot \tilde{F}_s \tag{14}$$

Equation (14) represent a differential equation which has to be solved together with equation (13). Because of the constraints from equation (13) the system will be non-linear and must be solved numerically. The solution has to be performed in phases because the roller drum may lift off from the ground and it may even make a whole cycle in the air without contact with the ground. The instants

when the solution enters another phase or state is not known in advance and has to be determined as part of the solution.

The elastic half space is characterised by the primary variable ***G***, the shear modulus of the material. The elastic material is further defined by the secondary parameters density ***r*** and Poisson's ratio ***n*** which have a smaller range of variation than ***G***. These parameters enter into the term H(s) in equation (14), deciding the static stiffness and the dynamic behaviour of the system.

The roller moves along the surface and it is assumed that the roller speed is high enough that the drum will hit fresh soil every cycle.

3. Numerical solution

The interaction between the drum and the soil passes different phases during the excitation cycles. The forces and the motions of the soil and the drum are described by different sets of equations in the different phases. The numerical solution is done in short time steps and the state of the system is checked in every step to decide if a change of state has occurred.

Three different states of the system are considered:

Loading. The plastic layer is successively deformed according to equation (13) and the load is transmitted through the plastic layer and applied as strip load with parabolic distribution to the surface of the elastic half space. The surface of the elastic half space is displaced according to equation (14). The drum is moving according to equations (11) and (12) and consistent with the soil contact force.

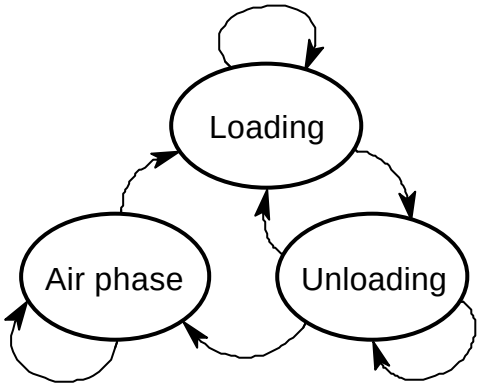

Figure 13: State diagram for numerical calculation.

Unloading. The plastic layer is not deformed further. The soil force applied by the drum is decreasing but there is still contact between the drum and the soil. The forces and displacements are determined by equations (11) and (14).

Air phase. The contact is lost between the drum and the soil. The drum and the soil move as two separate systems. This state may never occur if the excitation is low or the soil is very soft.

The different phases and the possible transitions between phases are illustrated by the state diagram of Figure 13. Each new time interval in the calculation represents a new state, that may or may not belong to the same phase.

The differential equations are transformed into difference equations using a constant time step Δt. An IIR-method is applied and the output value for a new time step is calculated as a weighted sum of the new input value and old output and input values. The weights are given by the coefficients of the difference equations. The number of old values involved is equal to the order of the differential equation being integrated.

The time step size necessary is dependant on the highest frequencies present in the results. A suitable value for Δt is one fifth of the shortest period of interest. The mapping of the transfer function to the z-plane causes a certain warp of the frequency scale that is corrected for.

Example of roller simulation

Input data

An example will be presented of typical results that can be obtained with the kind of simulation model that has been described. A typical 10 ton type self-propelled vibratory roller (Figure 9) will be simulated.

Roller data:

Frame	Mass acting vertically on the drum	2400 kg
Drum	Mass	3200 kg
	Diameter	1.50 m
	Width	2.10 m
Eccentric	Mass	50 kg
	Frequency	15 - 40 Hz
	Amplitude	0 - 2.5 mm

Soil data:

Density ρ = 2000 kg/m^3
Poisson's ratio ν = 0.25

There is a certain relationship between ***p*** and ***G*** . A weak soil having a low ***G*** will generally have a high value of ***p*** and vice versa. A typical co-variation of the two parameters are shown in Figure 14.

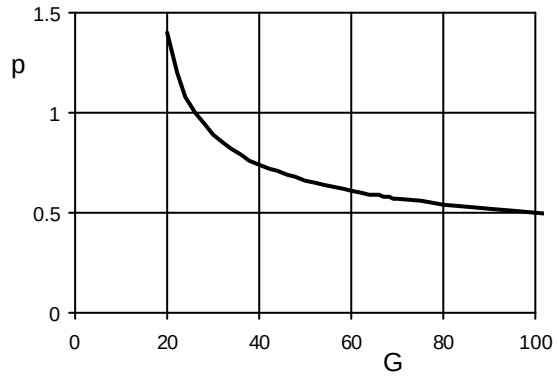

*Figure 14: Assumed co-variation of soil parameters **p** and **G** with varying degree of compaction.*

There will be considerable variation in this relationship for different soil conditions. A stiff layer on top of weak sublayers will for instance have a ***p*** that is below the curve in Figure 14.

The data for Figure 14 was obtained from test runs with the simulation program and comparison of simulated drum accelerations with recorded ones. When comparing different roller sizes the value of ***p*** has to be scaled to the radius of the drum.

Elastic transfer function:

A 2-pole approximation of Reissner functions for a rectangular area computed by Elorduy et al was used. In order to get better agreement with measured results, some internal damping was introduced. The calculated Q-value of 0.6 was decreased to 0.4.

The length/width-ratio of the loaded area differs from the one valid for Elorduy's data. When calculating the frequency scale for the actual loading area it was reshaped to the same length/width-ratio, while keeping the magnitude of the area unchanged.

Time step size:

The time step was selected to give 128 samples for one revolution of the eccentric shaft, which means that the size of the time step varies with the excitation frequency.

Simulation results

1. Drum accelerations

The simulated acceleration in the vertical direction is an important indicator of the validity of the simulation result. The acceleration is easy to measure on a roller and it is also used as the input signal for the calculation of various compaction meter values.

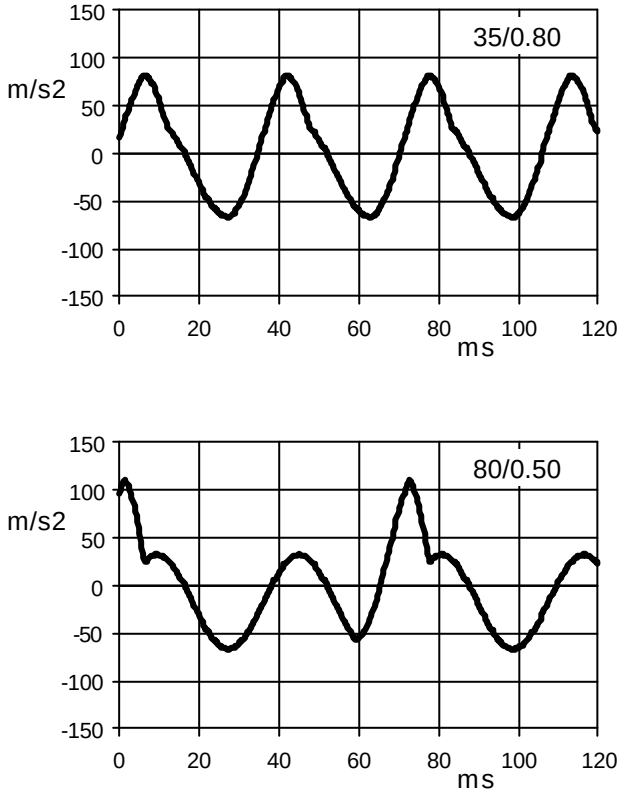

Figure 15: Simulated vertical drum accelerations. f=28 Hz, A=1.6 mm.

Figure 15 shows simulated results for two different soil conditions. The excitation frequency and amplitude have the nominal values for the roller, which are 28 Hz and 1.6 mm respectively.

In the first diagram (G=35 MPa, p=0.8 mm), the vibration is stable with the cycles repeating without change. There is a typical asymmetry caused by the drum lifting off of the ground during a certain part of each cycle. The drum hits the ground at a certain phase angle of the vibration, which causes the upwardly directed acceleration peak.

The second part of Figure 15 illustrates a situation with a stiffer soil (G=80 MPa, p=0.5 mm), when the roller is double-jumping. The drum hits the ground very hard every other cycle and gets such a heavy rebound, that it makes a full cycle in the air before hitting the ground again.

The vibration is stable, but is still not desirable for various reasons. Firstly the very heavy blows will hit the ground with double the normal separation and will cause reloosening of already compacted material. Secondly, the fundamental frequency of the drum vibration will be halved and at the same time the drum will become a very high amplitude. This will cause heavy excitation of the roller frame.

2. Vibration stability

Because of the non-linearities involved in the system, instability phenomena are likely to occur. When the excitation amplitude is increased, period doubling will show up, first as double jump as illustrated above and than as another doubling leading to quad jump i.e. a situation where the vibration pattern has a period of 4 full revolutions of the eccentric shaft. When the excitation exceeds a certain limit the vibration enters a chaotic state and the vibration will never repeat itself but will vibrate in a random manner.

It is important to know the conditions under which these instabilities appear. Instabilities can be investigated by running simulations for a large number of combinations of frequency and amplitudes and plotting the resulting vibration modes as in Figure 16.

These simulations are rather time consuming because the program has to be run for a fairly long time for each combination. The reason for this is that the vibration need many periods to settle to a stable state.

The instability visible to the left in the diagram at frequencies of 15-18 Hz is related to the drum/soil resonance. The frequency of this resonance decreases with the excitation amplitude, which is a well known fact confirmed by measurements (Kröber [13]).

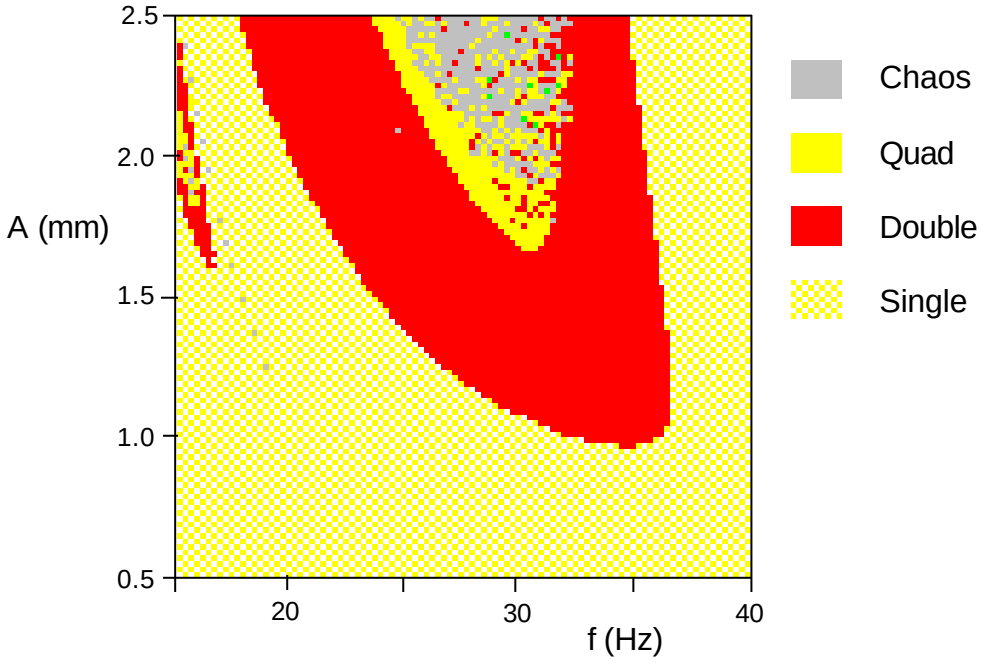

Figure 16: Vibration stability result for a soil with parameters G=80 MPa and p=0.5 mm.

3. Force/displacement results

One important application for the simulation program is the assessment of the compaction efficiency of the roller.

The compaction near the surface is accomplished by a displacement of the soil and is unfortunately also accompanied by a re-loosening of previously compacted soil volumes. This is a well known

disadvantage for vibratory rollers that is difficult to avoid. The loose upper layer often has to be compacted by a final static pass over the area.

The compaction effect on deeper layers is mainly caused by the creation of a vibration in the soil material. The vibration enables the grains to relocate into a more dense arrangement under influence by the combined effect of gravity and static load generated by the roller.

The simulation program generates output data for soil forces and displacements that can be used for an estimation of the compaction potential. By varying the parameters of the roller it is then possible to study the influence on compaction efficiency.

It is natural to present the results in the same way as the results from a plate load test, i.e. as drum displacement versus applied force. A few examples are shown in Figure 17.

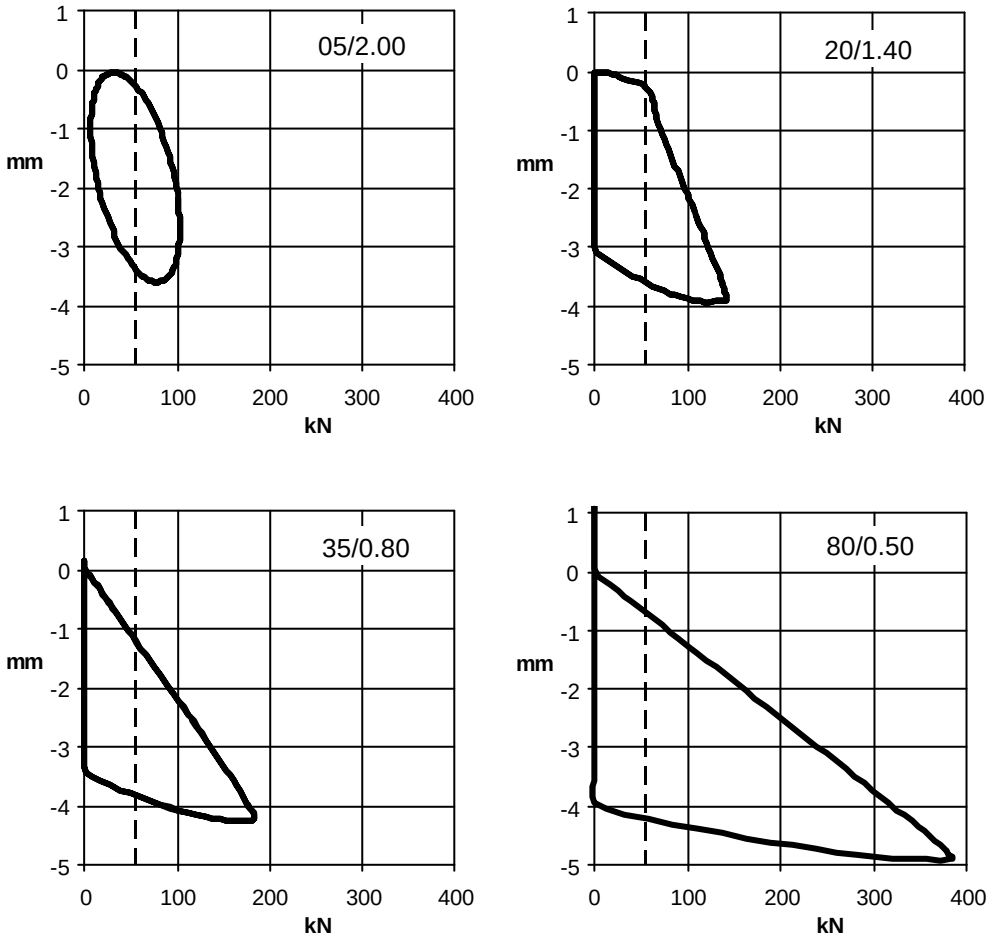

Figure 17: Drum displacement vs. soil force. The vertical dotted lines indicate the static load. f=28 Hz, A=1.6 mm.

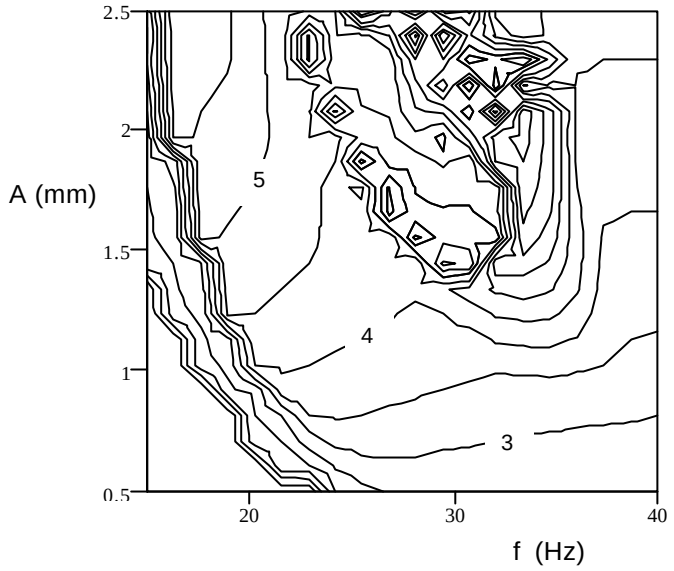

Figure 18: Maximum soil force in relation to the static force. G=80 MPa and p=0.5 mm.

The maximum force $F_{s\ max}$ transmitted to the soil is an interesting parameter. As seen in Figure 17, the maximum soil force in those examples vary from twice the static load to 6.9 times the static load. In the last case the force occurs only every other cycle with the drum doing a cycle in the air in between.

The ratio $F_{s\ max}$ / F_{stat} has been investigated further for the whole range of frequencies and amplitudes. In cases of double jump the value of the quotient is evaluated as an average value for a large number of cycles.

As seen from the contour plot in Figure 18 the value $F_{s\ max}$ / F_{stat} varies gradually from 3 to 6 in the area of stable vibration.

4. Compaction meter results

The simulation program delivers the necessary output signals for the calculation of CompactoMeter Values (CMV). An example of simulated CMV is shown in Figure 19. The low amplitude will never put the roller into double jump mode and the CMV are increasing monotonously with the stiffness of the soil.

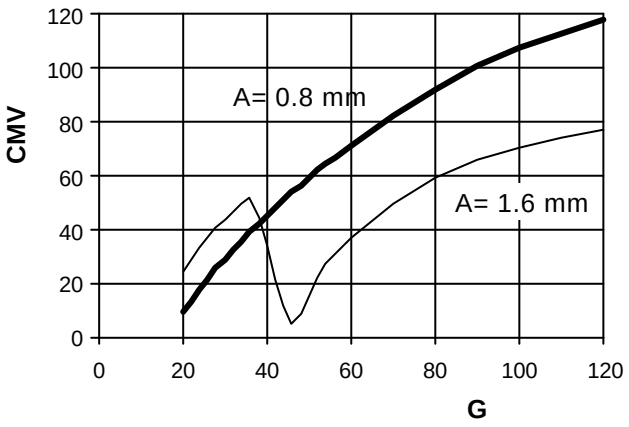

Figure 19: CMV vs. G for two different amplitudes. The value of the plastic parameter p was coupled to the value of G according to Figure 14.

The high amplitude on the other hand will force the roller into double jump mode and the CMV-curve will show a discontinuity. The value of CMV will then increase again monotonously as the stiffness increases, however, the value will never reach the level it has for the low amplitude.

It is evident from these results that it is very important, when using CMV for result verification, that the roller vibration is stable and takes place in the same mode and that the same amplitude is used as at the calibration .

CMV varies also with frequency, with all other parameters kept constant. The variation over the whole range of amplitudes and frequencies for a fixed combination of G and p is illustrated by Figure 20.

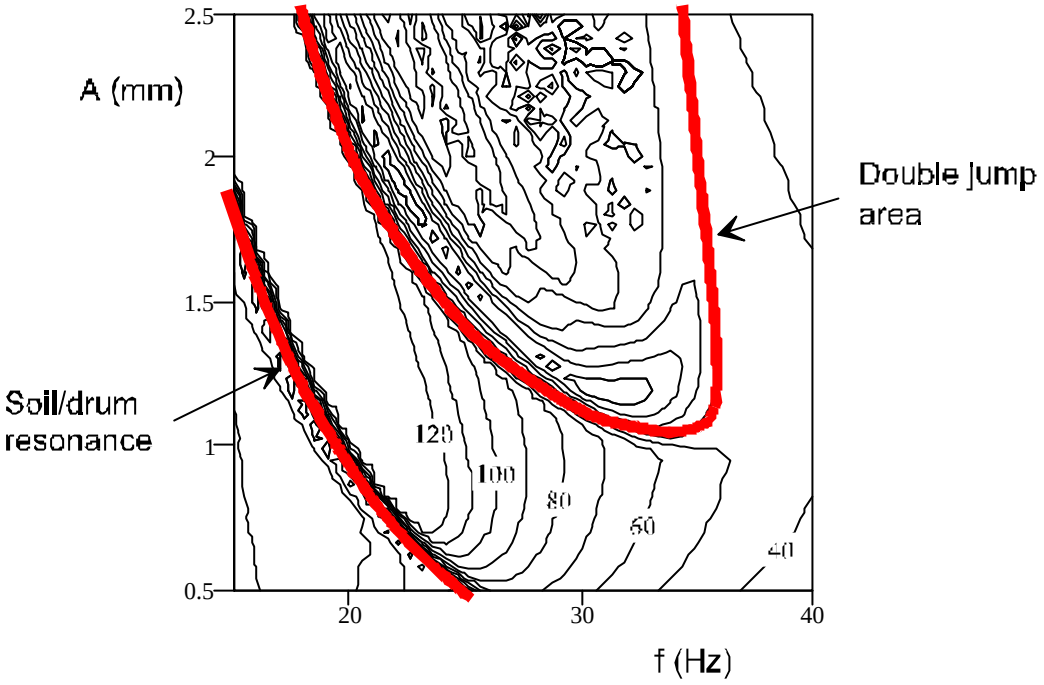

Figure 20: Variation of CMV with frequency and amplitude of the roller for constant soil conditions (G=80 MPa, p=0.5 mm)

Notation

α	length/width ratio of loaded area (=L/B)
A	nominal amplitude of the roller drum
a_0	dimensionless frequency (=dω/v_s)
a_x	horizontal drum acceleration
a_z	vertical drum acceleration
B	half width of loaded area
c	cohesive strength
CMV	Compaction Meter Value
d	characteristic linear dimension
D	dimensionless displacement
δ	vertical displacement
e	void ratio
f	excitation frequency
F_f F_s F_e	forces (frame, soil, exciter)
F_{stat}	static force
γ	unit weight
G G_{max}	shear modulus, initial shear modulus
H	transfer function
φ	internal friction angle
k	factor for calculating width of the loaded area
κ	static load factor
L	half length of loaded area
m_d	drum mass
ν	Poisson´s ratio
N_c N_q N_γ	bearing capacity factors
p	parameter for plastic deformation
Q Q_u	load, ultimate load
r	drum radius
ρ	density
σ_u	ultimate stress
v_s	shear wave velocity
ω	angular frequency
W	roller drum width
z_{se} z_{sp}	vertical soil displacement (elastic, plastic)

References

1. **Ahmad S., Bharadwaj A.** : *Horizontal Impedance of Embedded Strip Foundations in Layered Soil*. Journal of Geotechnical Engineering, ASCE, Vol. 117, No. 7, July 1991.

2. **Borja R.I. et al.** : *Nonlinear response of vertically Oscillating Rigid Foundations.* Journal of Geotechnical Engineering, ASCE, Vol. 119, No. 5, May 1993.

3. **Bycroft G. N.** : *Forced Vibrations of a Rigid Circular Plate on a Semi-infinite Elastic Space and on an Elastic Stratum.* Phil. Trans. of the Royal Society, London, Series A, Vol. 248, No. 948, 1956, pp. 327 - 368.

4. **Chen E.F., Davidson H.L.** : *Bearing Capacity Determination by Limit Analysis.* Journal of the Soil Mechanics and Foundations Division, ASCE, Vol. 99, No. SM6, June 1973.

5. **Dasgupta S. P., Rao K.** : *Dynamics of Rectangular Footings by Finite Elements.* Journal of the Geotechnical Engineering Division, ASCE, Vol. 104, No. GT5, Proc. Paper 13763, May, 1978, pp. 621-637

6. **Elorduy, J. . Nieto, J.A. , Szekely. E.M.** : *Dynamic Response of Bases of Arbitrary Shape Subjected to Periodic Vertical Loading.* Proc. of the International Symposium on Wave Propagation and Dynamic Properties of Earth materials, Univ. of New Mexico, Albuquerque, N.M. , August 1967, pp. 105-121.

7. **Forssblad L.** : *Vibratory Soil and Rock Fill Compaction*, Dynapac Maskin AB, 1981.

8. **Gazetas G. et al.** : *Vertical response of Arbitrarily Shaped Embedded Foundations.* Journal of Geotechnical Engineering, ASCE, Vol. 111, No. 6, June 1985.

9. **Grabe J.** : *Experimentelle und theoretische Untersuchungen zur flächendeckenden dynamischen Verdichtungskontrolle.* Dissertation. Veröffentlichung des Institutes für Bodenmechanik und Felsmechanik, Universität Karlsruhe, Heft 123, 1992.

10. **Hardin B.O., Richart F.E.** : *Elastic Wave Velocities in Granular Soils.* Journal of the Soil Mechanics and Foundations Division, ASCE, Vol. 89, No. SM1, February, 1963.

11. **Hsieh T.K.** : *Foundation Vibrations*. Proceedings Institution of Civil Engineering, London, Vol. 22, 1962.

12. **Karafiath L.L., Nowatzki E.A.** : *Soil Mechanics for Off-road Vehicle Engineering.* Trans Tech Publications, Series on Rock and Soil Mechanics, Vol. 2, No. 5, 1978.

13. **Kröber W.** : *Untersuchung der dynamischen Vorgänge bei der Vibrationsverdichtung von Böden.* Dissertation. Schriftenreihe des Lehrstuhls und Prüfamtes für Grundbau, Bodenmechanik und Felsmechanik der TU München, Heft 11, 1988.

14. **Lysmer J., Richart F.E. Jr** : *Dynamic Response of Footings to vertical Loading*. Journal of the Soil Mechanics and Foundations Division, ASCE, Vol. 92, No. SM1, January, 1966.

15. **Machet J.M.** : *Interprétation de l´efficacité des compacteurs vibrants.* Rapport de recherche No 59, Laboratoires Central des Ponts et Chaussées, Paris, 1976.

16. **Meek J.W, Wolf J.P.** : *Approximate Green´s Function for Surface Foundations*. Journal of the Geotechnical Engineering Division, ASCE, Vol. 119, No. 10, Oct. 1993.

17. **Nii, Y.** : *Experimental Half Space Dynamic Stiffness.* Journal of Geotechnical Engineering, ASCE, Vol. 113, No. 11, Nov. 1987.

18. **Öner M.** : *A Finite Element Approach to the Equivalent Spring Constant Problem in Soil dynamics.* Soil Mechanics and Foundation Engineering Division, The Norwegian Institute of Technology, Trondheim, Norway, August 1975.

19. **Pietzsch, D.** : *Untersuchungen zum Schwingungsverhalten und zur Verdichtungswirkung von Vibrationswalzen.* Fortschr.-Ber. VDI Reihe 4, Nr. 108, Düsseldorf, VDI-Verlag 1991.

20. **Quinlan P.** : *The Elastic theory of Soil Dynamics.* Symposium on Dynamic Testing of Soils, Atlantic City, N.J., 1953. ASTM Special Tech. Publ. No. 156.

21. **Reissner V.E.** : *Stationäre, Axialsymmetrische, durch eine Schüttelnde Masse Erregte Schwingungen eines Homogenen Elastischen Halbraumes*. Ingenieur-Archiv, VII Band, pp. 381-396, 1936.

22. **Richart F.E., Woods R.D., Hall J.R.** : *Vibrations of Soil and Foundations.* Prentice-Hall, Inc., Englewood Cliffs, N.J., 1970.

23. **Sung T.Y.** : *Vibrations in Semi-infinite Solids due to Periodic Surface Loading.* Symposium on Dynamic Testing of Soils, Atlantic City, N.J., 1953. ASTM Special Tech. Publ. No. 156.

24. **Széchy K.** : *Der Einfluss der Sohlflächenform von Streifenfundamenten auf die Tragfähigkeit und Spannungsausbreitung.* Verein Deutscher Ingenieure - Zeitschrift, Vol. 109, Nr.8, 1967, pp. 339-344.

25. **Veletsos A., Verbic B.** : *Basic Response Functions for Elastic Foundations.* Journal of the Engineering Mechanics Division, ASCE, Vol. 100, No. EM2, April, 1974.

26. **Vesic A. S.** : *Analysis of Ultimate Loads of Shallow Foundations.* Journal of the Soil Mechanics and Foundations Division, ASCE, Vol. 99, No. SM1, January, 1973.

27. **Vrettos C., Prange, B.** : *Evaluation of In Situ Effective Shear Modulus from Dispersion Measurements.* Journal of Geotechnical Engineering, ASCE, Vol.116, No.10, October 1990.

28. **Yoo, T. Selig, E.T.** : *Dynamics of Vibratory Roller Compaction.* Journal of the Geotechnical Engineering Division, ASCE, No.105, 1979, pp. 1211-1231.